




Identification of two *Bacillus thuringiensis* Cry3Aa toxin-binding aminopeptidase N from *Rhynchophorus ferrugineus* (Coleoptera: Curculionidae)

Research Paper

*These authors contributed equally.

Shaozhen Wang^{1,2,*}, Yajie Guo^{1,3,4,*}, Yunzhu Sun^{1,3}, Mingqing Weng^{1,3}, Qiliao Liao¹, Ru Qiu¹, Shuangquan Zou¹ and Songqing Wu^{1,3,5} 

Cite this article: Wang S, Guo Y, Sun Y, Weng M, Liao Q, Qiu R, Zou S, Wu S (2023). Identification of two *Bacillus thuringiensis* Cry3Aa toxin-binding aminopeptidase N from *Rhynchophorus ferrugineus* (Coleoptera: Curculionidae). *Bulletin of Entomological Research* **113**, 615–625. <https://doi.org/10.1017/S0007485323000299>

¹College of Forestry, Fujian Agriculture and Forestry University, Fuzhou 350000, China; ²CAS Key Laboratory of Insect Developmental and Evolutionary Biology, CAS Center for Excellence in Molecular Plant Sciences, Chinese Academy of Sciences, Shanghai 200032, China; ³Key Laboratory of Integrated Pest Management in Ecological Forests, Fujian Province University, Fujian Agriculture and Forestry University, Fuzhou 350000, China; ⁴Asian Research Center for Bioresource and Environmental Sciences, Graduate School of Agricultural and Life Sciences, The University of Tokyo, Tokyo 188-0002, Japan and ⁵State Key Laboratory of Ecological Pest Control for Fujian and Taiwan Crops, College of Forestry, Fujian Agriculture and Forestry University, Fuzhou, China, 350002

Received: 4 April 2023
Revised: 13 June 2023
Accepted: 19 June 2023
First published online: 19 July 2023

Keywords:
Aminopeptidase N; Cry3Aa toxin; interaction mechanism; *Rhynchophorus ferrugineus*

Corresponding author:
Songqing Wu;
Email: dabinyang@126.com

Abstract

Rhynchophorus ferrugineus is a quarantine pest that mainly damages plants in tropical regions, which are essential economic resources. Cry3Aa has been used to control coleopteran pests and is known to be toxic to *R. ferrugineus*. The binding of the Cry toxin to specific receptors on the target insect plays a crucial role in the toxicological mechanism of Cry toxins. However, in the case of *R. ferrugineus*, the nature and identity of the receptor proteins involved remain unknown. In the present study, pull-down assays and mass spectrometry were used to identify two proteins of aminopeptidase N proteins (RfAPN2a and RfAPN2b) in the larval midguts of *R. ferrugineus*. Cry3Aa was able to bind to RfAPN2a ($K_d = 108.5$ nM) and RfAPN2b ($K_d = 68.2$ nM), as well as midgut brush border membrane vesicles ($K_d = 482.5$ nM). *In silico* analysis of both RfAPN proteins included the signal peptide and anchored sites for glycosyl phosphatidyl inositol. In addition, RfAPN2a and RfAPN2b were expressed in the human embryonic kidney 293T cell line, and cytotoxicity assays showed that the transgenic cells were not susceptible to activated Cry3Aa. Our results show that RfAPN2a and RfAPN2b are Cry3Aa-binding proteins involved in the Cry3Aa toxicity of *R. ferrugineus*. This study deepens our understanding of the action mechanism of Cry3Aa in *R. ferrugineus* larvae.

Introduction

Rhynchophorus ferrugineus is quarantined internationally and threatens plants in tropical areas that are essential economic resources, such as *Phoenix canariensis*, *Cocos nucifera* and *Areca catechu* (Dembilio *et al.*, 2009; Huang, 2013). *R. ferrugineus* is a swarming trunk borer with a long larval phase that is mainly concealed in the xylem and phloem of palm trees, destroying the internal tissues (Llácer *et al.*, 2010). Currently, it has invaded Oceania, Asia, Africa, the United States, and the area covered by the European and Mediterranean Plant Protection Organization, causing severe economic loss and ecological damage (Al-Ayedh, 2008; Bozbuga and Hazir, 2008). Currently, chemical pesticides are mostly used to control *R. ferrugineus*; however, the dangers of chemical pesticides to the environment, humans and animals, as well as the evolution of pest resistance, have restricted their usage (Han *et al.*, 2013; Chen, 2016). The management of *R. ferrugineus* is gradually transitioning to the use of ecologically friendly microbial insecticides that are safe for humans and animals.

Bacillus thuringiensis is a ubiquitous gram-positive rod-shaped bacterium with insecticidal activity against over 3000 larvae of different insect orders, accounting for 2% of the insecticidal market (Schnepf *et al.*, 1998; Bravo *et al.*, 2011). During spore formation, *B. thuringiensis* produces toxins from parasporal crystals, mainly Cry and Cyt crystals (Bravo *et al.*, 2007). The Cry family has broader insecticidal activity than the anti-dipteran properties of Cyt toxins. Cry3, Cry7 and Cry8 were found to be active against Coleopteran larvae (Ibrahim *et al.*, 2010; Crickmore *et al.*, 2021). Cry3Aa was the first toxin found to be toxic to Coleoptera and was weakly toxic to *R. ferrugineus* (Guo *et al.*, 2021). Therefore, their field applications are limited. The mechanism-based modification of existing Cry toxins is one of the most crucial techniques for developing highly virulent toxins for non-Bt target insects (Guo *et al.*, 2011). Therefore, understanding the action mechanisms of non-Bt target toxins is critical.

The mode of action of Cry toxins has been extensively studied. Once ingested by the target insect, crystals are dissolved in the intestinal fluid and activated by digestive enzymes. The activated toxin then binds to receptors on midgut brush border membrane vesicles (BBMVs), oligomerizes, and is inserted into the cell membrane, finally causing insect death Adang *et al.* (2014). Binding receptors are necessary for the toxin to exert its virulence throughout the process (Bravo *et al.*, 2013). Midgut-binding receptor species of Cry toxins have been identified in major agroforestry pests, including cadherin-like proteins, aminopeptidase N (APN), alkaline phosphatase (ALP) and the ABC transporter family (Soberón *et al.*, 2018; Sato *et al.*, 2019). Many Coleopteran receptors for Cry3Aa have been identified, including the ABCB transporter from *Leptinotarsa decemlineata*, APN from *Monochamus alternatus* and TmCad1 from *Tenebrio molitor* (Fabrick *et al.*, 2009; Guo *et al.*, 2020; Güney *et al.*, 2021). Moreover, it is feasible to develop receptor action models using exogenous eukaryotic expression systems. For example, human embryonic kidney 293T cells (HEK293T) expressing BtR175b from *Bombyx mori* showed swelling and death after treatment with Cry1Aa, indicating that this receptor is indispensable (Tsuda *et al.*, 2003). However, the Cry3Aa-binding receptor in the midgut of *R. ferrugineus* remains unknown.

Therefore, in this study, potential Cry3Aa-binding proteins on BBMVs from *R. ferrugineus* were preliminarily screened using ligand blotting, pull-down assays and mass spectrometry analyses. Western blotting and enzyme-linked immunosorbent assays (ELISA) were performed to determine the ability of Cry3Aa to bind to RfAPNs. An *in vitro* validation environment was established to confirm the function of RfAPNs using the MTT assay and morphological observations. This study elucidated the toxicological mechanism of the Cry3Aa toxin in *R. ferrugineus* larvae and provided a theoretical basis for biological control.

Materials and methods

Insect rearing and cell line

The larvae of *R. ferrugineus* were maintained in the Key Laboratory of Integrated Pest Management in Ecological Forests, Fujian Agriculture and Forestry University, at 28°C and 70% humidity with 12-h light/12-h dark cycles. HEK293T cells were cultured in Dulbecco's modified Eagle medium (Biological Industries, Beit-Haemek, Israel) containing 10% foetal bovine serum (Biological Industries, Beit-Haemek, Israel) in a humidified 5% CO₂ atmosphere at 37°C.

Extraction of BBMVs from the midgut

BBMVs from the three-instar larvae of *R. ferrugineus* were extracted using a previously published method (Wolfersberger *et al.*, 1987). Briefly, a sample of second instar larvae midgut (0.1 g) was homogenized in 500 µl of pre-chilled Buffer A (0.3 mol l⁻¹ mannitol, 5 mM ethylene glycol tetraacetic acid, 17 mmol l⁻¹ Tris-HCl, pH 7.5) with 5 µl of 1 mmol l⁻¹ phenylmethanesulfonyl fluoride (PMSF) protease inhibitor. The homogenate was transferred to a new tube, and an equal volume of 24 mM MgCl₂ was added, followed by incubation on ice for 15 min. Thereafter, it was centrifuged at 4°C, 2500 × g for 15 min. The supernatant was stored in a new tube, and the precipitate was resuspended in 500 µl of Buffer A containing 5 µl of PMSF. This procedure was repeated three times. The supernatants were

collected and centrifuged at 30,000 × g for 30 min at 4°C. The pellet was resuspended in 100 µl of Buffer A containing PMSF to obtain solubilized BBMVs proteins. The protein concentration was determined using the Bradford assay (Sangon Biotech, Shanghai, China), and the extractive quality was analysed using SDS-PAGE.

Cry3Aa toxin preparation

The glutathione-S-transferase (GST)-Cry3Aa protein was purified for the ligand blot and pull-down assay using the pGEX-KG-Cry3Aa *Escherichia coli* BL21 strain stored in the laboratory. First, the bacteria were incubated in Luria-Bertani medium containing 100 µg ml⁻¹ ampicillin until the OD₆₀₀ reached 0.6. Isopropyl-β-D-galactopyranoside was then added (to a final concentration of 0.8 mM) and cultured in a shaker at 16°C for 48 h. The *E. coli* cells were collected following centrifugation at 10,000 × g for 10 min at 4°C, followed by resuspension using phosphate-buffered saline (PBS) buffer (2.7 mmol l⁻¹ KCl, 140 mmol l⁻¹ NaCl, 1.8 mmol l⁻¹ KH₂PO₄, 10 mmol l⁻¹ Na₂HPO₄, pH 7.3) and centrifugation again at 10,000 × g for 10 min at 4°C. Ultrasonic cell disruption was performed using a mixture of ice and water. Cry3Aa was purified from the supernatant using Glutathione Sepharose 4 B (G.E. Healthcare, Waltham, MA, USA) according to manufacturer's instructions.

A Cry3Aa crystal protein was extracted from the *B. thuringiensis* pHT304-Cry3Aa BMB171 stored in our laboratory. In brief, the bacteria were cultured in a pericyte medium (2 g l⁻¹ yeast extract, 10 g l⁻¹ tryptone, 1 g l⁻¹ KH₂PO₄, 0.02 g l⁻¹ FeSO₄·7H₂O, 0.3 g l⁻¹ MgSO₄·7H₂O, 0.02 g l⁻¹ MnSO₄·7H₂O, 0.02 g l⁻¹ ZnSO₄·7H₂O, pH 7.0) for 60 h at 30°C. The cell pellet was collected after centrifugation at 10,000 × g for 10 min at 4°C and washed three times with 1 mol l⁻¹ NaCl and double-distilled water. Purified inclusions were solubilized with solution I (50 mmol l⁻¹ Na₂CO₃, 10 mmol l⁻¹ DL-dithiothreitol, pH 11) for 4 h at 4°C. After centrifugation at 10,000 × g at 4°C for 10 min, the insoluble materials were removed. Crystal protein was obtained from the supernatant by adjusting the pH to 4.3 with acetic acid and centrifuging at 10,000 × g at 4°C for 10 min. The protein was washed with double-distilled water three times, solubilized in 50 mmol l⁻¹ NaHCO₃ (pH 10.0) and stored at -80°C for future analysis. Protein concentrations were measured using the Bradford assay (Sangon).

Ligand blot assay for BBMVs

BBMVs (20 µg) were separated by 10% sodium dodecyl sulphate-polyacrylamide gel electrophoresis (SDS-PAGE) and transferred onto a nitrocellulose membrane (Millipore, Bedford, MA USA) (200 mA, 80 min). The membrane was blocked in Tris buffer saline (TBST; 20 mmol l⁻¹ Tris-HCl, 150 mmol l⁻¹ NaCl, 0.05% Tween-20, pH 7.4) containing 5% skim milk powder overnight at 4°C. After washing three times with TBST, the membrane was probed with 20 µg ml⁻¹ Cry3Aa protein in TBST at 4°C for 3 h. Unbound proteins were removed by washing the membrane three times. A primary rabbit polyclonal antibody specific to Cry3Aa (1:2000 dilution) was used to incubate the membrane at 37°C for 1 h, followed by incubation with a secondary goat anti-rabbit IgG antibody conjugated with DyLight 488 (1:5000; Thermo Fisher Scientific, Waltham, MA USA). Immunoreactive bands to Cry3Aa were detected using a Syngene GBOX-CHEMI-XT4 system (Syngene, Cambridge, UK). The Cry1Ac

toxin was used as a negative control because Coleopteran insects are not susceptible to Cry1Ac and lack functional receptors for the toxin (de Oliveira *et al.*, 2023).

Pull-down assay and mass spectrometry

A pull-down assay was conducted to screen Cry3Aa-binding proteins in BBMV as described by Guo *et al.* (2020). In brief, 40 μl of GST-Cry3Aa-Glutathione Sepharose 4B was incubated in 200 μg BBMVs at 4°C for 1 h with gentle rocking. Unbound proteins were removed by centrifugation at 3000 $\times g$ for 5 min at 4°C. The beads were washed ten times using PBS and 1 mol l^{-1} NaCl, and then washed with PBS to reduce the concentration of NaCl. Finally, the proteins were denatured with 50 μl of SDT lysis buffer (2% SDS, 100 mmol l^{-1} DTT, 100 mmol l^{-1} Tris-HCl, pH 7.6) at 100°C and analyzed using 10% SDS-PAGE. GST-Cry1Ac-binding BBMVs were used as negative controls, using the same procedure. The separated bands were processed for mass spectrometry using an Orbitrap-Fusion-Tribrid mass spectrometer (Thermo Scientific, Waltham, MA, USA). The obtained sequences were compared with the *R. ferrugineus* larval transcriptome database (PRJNA933083) to identify putative binding proteins.

Protein structures and docking simulation

To determine the structural features of the proteins, we predicted the O- and N-glycosylation sites, the signal peptide and the three-dimensional model structures using NetOGlyc v1.0 (<http://www.cbs.dtu.dk/services/NetOGlyc/>), NetNGlyc v1.0 (<http://www.cbs.dtu.dk/services/NetNGlyc/>), SignalP-6.0 (<https://services.healthtech.dtu.dk/service.php?SignalP>) and SWISS-MODEL (<https://www.swissmodel.expasy.org/>) software. To investigate the interaction between Cry3Aa and RfAPNs, Dock Proteins (ZDOCK) software was used to analyse molecular docking using Discovery Studio 2016 (Chen and Weng, 2002). In addition, homology analyses of RfAPNs were performed using the NCBI protein-protein BLAST (<https://blast.ncbi.nlm.nih.gov/Blast.cgi>). The retrieved APN protein sequences were aligned using ClustalW. Neighbour-joining trees were constructed and adjusted using MEGA X software and Evolview v3 (Kumar S *et al.*, 2018; Subramanian *et al.*, 2019).

Expression constructs

We obtained full-length cDNA sequences of *Rfapn2a* and *Rfapn2b* from the mass spectrometry results. After gene synthesis (Synbio Technologies, Suzhou, China), the *Rfapn2a* coding sequence (CDS) was amplified using specific primers (forward primer: 5'-ATCTGGTTCCGCGTggatccATGGATTACATTTTGGGATTG-3'; reverse primer: 5'-CCACCGGAAATTTCCCGggatccTTATTCTTGATAATTTAAAC-3'). The *Rfapn2b* gene was obtained by digestion with the restriction enzymes *Bam*HI and *Sal*I. The products were purified using an E.Z.N.A.® Gel Extraction Kit (OMEGA, Norcross, Georgia, USA). The two fragments were inserted into pGEX-KG, and *E. coli* BL21 was transformed. The expression and purification of recombinant RfAPN2a and RfAPN2b proteins were conducted similarly to those of GST-Cry3Aa. Simultaneously, the proteins were biotinylated using the EZ-Link™ NHS-Biotin (Thermo Scientific, Waltham, MA, USA) following manufacturer's instructions. Next, *Rfapn2a* and *Rfapn2b* were amplified using a PCR with

specific primers (listed in Table S1) and infusion-cloned into the pQCMV eukaryotic expression vector encoding the FLAG + EGFP epitope tags at the *Kpn*I site. The constructed plasmids were transformed into *E. coli* DH5 α .

Western blotting and far-western blotting

For western blot analysis, purified Cry3Aa toxins (73 kDa) and biotinylated APN proteins (134 kDa) were separated using 10% SDS-PAGE and transferred to nitrocellulose membranes (Millipore). The membranes were blocked with 5% skim milk in PBST (8 mmol l^{-1} $\text{Na}_2\text{HPO}_4 \cdot 12\text{H}_2\text{O}$, 0.136 mol l^{-1} NaCl, 2 mmol l^{-1} KH_2PO_4 , 2.6 mmol l^{-1} KCl, 0.05% Tween-20, pH 7.4) at 4°C overnight. After washing three times with PBST, the membranes with biotinylated APNs were incubated with streptavidin conjugated to horseradish peroxidase (HRP) (1:3000 dilution, Bioss, Beijing, China) for 1 h and then visualized using ECL chemiluminescence kits (Beyotime, Shanghai, China) according to manufacturer's protocol. The membrane with Cry3Aa was incubated with a primary rabbit polyclonal antibody against Cry3Aa (1:2000), followed by incubation with a secondary goat anti-rabbit antibody conjugated with DyLight 488 (1:5000). Binding was detected using the GBOX-CHEMI-XT4 system (Syngene).

As reported previously, protein-protein interactions were analyzed using far-western blotting (Einarson *et al.*, 2007). Purified RfAPN2a and RfAPN2b were separated using 10% SDS-PAGE and transferred to a nitrocellulose membrane (Millipore). After overnight incubation with blocking buffer (5% skim milk in PBST) at 4°C, the membrane was probed with purified Cry3Aa in PBST containing 0.1% BSA at 25°C for 2 h. Unbound proteins were removed by washing three times with PBST. The membrane was then incubated with a primary rabbit polyclonal antibody against Cry3Aa (1:2000) and goat anti-rabbit secondary antibody conjugated with DyLight 488 (1:5000). Antibody binding was visualized using the GBOX-CHEMI-XT4 system (SynGene). Similarly, Cry3Aa was transferred to nitrocellulose membranes (Millipore) and probed with purified biotinylated RfAPN2a and RfAPN2b proteins. The binding of interacting proteins was detected using the biotin antibody streptavidin/horseradish peroxidase (1:3000).

Enzyme-linked immunosorbent assay

To confirm the binding affinities of Cry3Aa to BBMVs and RfAPNs, ELISA were performed as previously reported (Pérez *et al.*, 2005). The ELISA plates were coated with 4 $\mu\text{g well}^{-1}$ of purified BBMVs, RfAPN2a and RfAPN2b proteins diluted in 0.05 mol l^{-1} Na_2CO_3 at 4°C overnight, washed with PBST three times and then incubated with blocking buffer (PBST, 5% skim milk) for 2 h at 37°C. After washing with PBST, Cry3Aa protein with gradient concentrations (0–2560 nM) in 100 μl of PBST were transferred to the BBMVs-coated plates, and 0–1280 nM Cry3Aa were transferred to the RfAPNs-coated plates and then incubated at 37°C for 2 h. Unbound proteins were removed and the plates were washed three times with PBST. Bound Cry3Aa was detected by incubation with primary rabbit polyclonal Cry3Aa antibody (1:2000 dilution) for 2 h and secondary goat anti-rabbit antibody conjugated with HRP (1:3000) for 1.5 h. TMB chromogen solution (Beyotime, Shanghai, China) was used under dark conditions in each well and kept at 37°C for 15 min, and 2 mol l^{-1} H_2SO_4 was applied to terminate the

reaction. The absorbance was measured at 450 nm using a Multiskan FC microplate reader (Thermo Scientific, Waltham, MA, USA). Experiments were performed in triplicate. Data were analyzed using GraphPad Prism 8 and SPSS 22 with a one-way ANOVA. The concentration corresponding to the half-maximal absorbance was considered the dissociation constant (Batool *et al.*, 2019).

Expression of RfAPN2a and RfAPN2b in HEK293T cells

HEK293T cells were cultured in a 6-well plate at approximately 60% confluence and transfected with pQCMV, pQCMV-*Rfapn2a* and pQCMV-*Rfapn2b* plasmids using a calcium phosphate precipitation protocol, as described by Wang *et al.* (2016). Briefly, for each transfection, 2 μ g endotoxin-free plasmid DNA was mixed with 2.5 mol l⁻¹ CaCl₂ (1/20 of total volume) and 2 \times HeBS (250 mmol l⁻¹ NaCl, 10 mmol l⁻¹ KCl, 1.5 mmol l⁻¹ Na₂HPO₄, 12 mmol l⁻¹ dextrose and 50 mmol l⁻¹ HEPES pH 7.5, pH adjusted to 7.05) and kept at room temperature for 5 min. The medium was discarded, and the DNA mixture was gently added to each well. Next, 2 ml of medium containing 25 μ M chloroquine was added to each well. After incubation at 37°C overnight, the medium was changed to a fresh medium without chloroquine and placed for 24 h to harvest cells for total RNA extraction. Real time (RT)-PCR was used to confirm the transfection results, and the primers used to amplify the cDNA fragments are listed in Table S1.

Cytotoxicity assays

The Cry3Aa crystal protoxin was activated using trypsin at a trypsin/protoxin ratio of 1/30 (w/w) at 37°C for 4 h. The activated toxin was dialyzed with PBS (Biological Industries Beit-Haemek, Israel) using Amicon® Ultra centrifugal filters (10 kDa, Merck Millipore, Darmstadt, Germany) for the cell viability assay, according to manufacturer's instructions. The HEK293T cells were cultured in 96-well plates. Until the HEK293T cells reached 60% confluence, the expression vectors for EGFP, RfAPN2a and RfAPN2b were transfected as described above. Each well was then filled with a series of concentrations of activated Cry3Aa (0, 12, 25, 50, 100 and 200 μ g ml⁻¹) diluted in 100 μ l of the culture medium. Three replicates were used for each cell line. After 6 h of incubation at 37°C, 10 μ l of 5 mg ml⁻¹ MTT was added and incubated for 4 h. 100 μ l of formazan solution was added and kept at 37°C incubator for 4 h to dissolve the crystal. The absorbance was measured at 570 nm. All values were calculated for control cells (considered 100%). To observe morphological changes, the transfected cells were cultured in a 24-well plate and incubated for 6 h with 200 μ M Cry3Aa solubilized in PBS (pH 7.4). Cells were incubated with PBS as a control. The cells were visualized and images were obtained using an inverted fluorescence microscope (TS-100; Nikon, Tokyo, Japan).

Results

Binding of Cry3Aa to *R. ferrugineus* BBMVs

BBMVs from *R. ferrugineus* larvae were extracted, and the GST-Cry3Aa protein was purified from the pGEX-KG-Cry3Aa *E. coli* BL21 strain (fig. 1a). Compared to Cry1Ac, which is non-toxic to Coleoptera, Cry3Aa was able to bind specifically to several proteins (~70, 100, 135 and 180 kDa) on *R. ferrugineus* BBMVs

(figs. 1b, c and S1). ELISA results showed that BBMVs binding positively correlated with the concentration of Cry3Aa, and the binding ability was saturated after treatment with 640 nM Cry3Aa ($K_d = 482.5$ nM). In addition, compared with Cry3Aa at 0 nM, the protein-bound OD₄₅₀ of BBMVs treated with different concentrations of Cry3Aa showed significant differences (fig. 1d).

Identification of Cry3Aa-binding proteins in *R. ferrugineus* larvae

A pull-down assay was performed to identify the Cry3Aa-binding proteins in the midgut of *R. ferrugineus* larvae, and the protein bands were analyzed by mass spectrometry (fig. 2a). Three protein types were able to bind to the Cry3Aa toxin: APN (RfAPN2a (Cluster-7879.9674) and RfAPN2b (Cluster-7879.8243), V-type proton ATPase catalytic subunit and GTP-binding protein (fig. 2b). A phylogenetic tree analysis revealed that the complete APN sequences obtained from GenBank formed eight clusters, and both RfAPNs clustered in APN2 (Class 2) (fig. 3). Bioinformatics analysis predicted that RfAPN2a and RfAPN2b had N-terminal signal peptides (Fig. S2). In addition, they contained multiple potential N-glycosylation and O-glycosylation sites, particularly RfAPN2a (Fig. S2).

To investigate the interaction of Cry3Aa with the RfAPN2a and RfAPN2b proteins of *R. ferrugineus*, molecular docking of Cry3Aa with the two binding proteins showed that Cry3Aa was able to bind to both RfAPN2a and RfAPN2b through two distinct but partially overlapping interfaces (Fig. S3). The binding sites in Cry3Aa were concentrated in domains II and III (fig. 4a, c). In addition, the predicted binding sites for Cry3Aa were mainly 300–600 amino acid residues for RfAPN2a and 0–200 amino acid residues for RfAPN2b (fig. 4b, d). We found that N62, D63, N515 and N545 in RfAPN2a and N77-T82 in RfAPN2b were not only glycosylation sites but also docking sites. And based on the interaction data, the area of contact interface between Cry3Aa and RfAPN2b was 750.98 Å², slightly greater than that between Cry3Aa and RfAPN2a (701.12 Å²).

Characterization of binding between Cry3Aa and recombinant RfAPNs

To test the binding ability of Cry3Aa to RfAPNs, the Cry3Aa crystal protein from *B. thuringiensis* acrySTALLIFEROUS strain BMB171, encoding the *cry3Aa* gene, was purified with a molecular weight of 73 kDa (fig. 5a, b). And we cloned full-length *Rfapn2a1* (2919 bp) and *Rfapn2b* (2868 bp) genes into a pGEX-KG vector and transformed them into *E. coli* BL21 competent cells. The purified GST-RfAPN2a and GST-RfAPN2b fusion proteins had molecular weights of 134 kDa (fig. 5c–e). The 134 kDa bands of RfAPN2a and RfAPN2b were checked and observed using a rabbit polyclonal antibody specific to Cry3Aa after the membranes were probed with the Cry3Aa toxin (fig. 5f, h). Similarly, the 73 kDa Cry3Aa was detected by the streptavidin antibody after blotting with biotinylated RfAPN2a and RfAPN2b (fig. 5g, i). Furthermore, ELISA results showed that more Cry3Aa bound to the immobilized RfAPNs with increasing concentrations of the Cry3Aa protein. The binding ability of RfAPN2a with Cry3Aa became saturated after treatment with 320 nM Cry3Aa ($K_d = 108.5$ nM), whereas that of the RfAPN2b protein was 160 nM ($K_d = 68.2$ nM). Compared to 0 nM Cry3Aa, the protein-bound

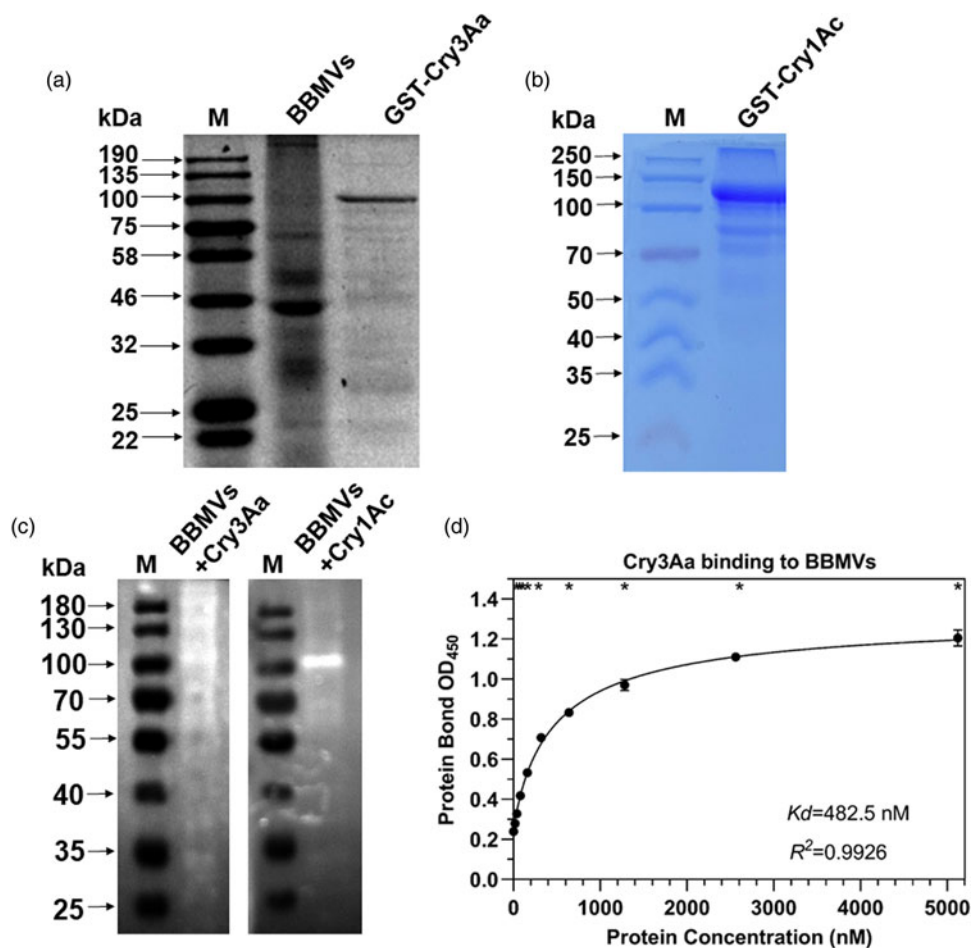


Figure 1. Cry3Aa toxin binding to the BBMVs of *Rhynchophorus ferrugineus*. (a and b) SDS–PAGE analysis of extraction of BBMVs, GST-Cry3Aa and GST-Cry1Ac. (c) Ligand blot analysis of Cry3Aa and Cry1Ac toxin to BBMVs, Cry1Ac toxin was used as a control. (d) The binding of Cry3Aa toxin to BBMVs was detected in the presence of increasing concentrations of Cry3Aa. Each point represents the mean of three independent measurements presented as $OD_{450} \pm$ standard error of the mean (SEM), and the lines represent the nonlinear regression for one-site binding. * Designates statistical significance at $P < 0.05$.

OD_{450} of RfAPNs with different concentrations of Cry3Aa was significantly different (fig. 6).

Cytotoxic effects of Cry3Aa on RfAPN2a or RfAPN2b-expressing HEK293T cells

Rfapn2a and *Rfapn2b* were transfected into HEK293T cells and the expressed proteins (Fig. S4). MTT assays indicated that the survival rate of all cells decreased with an increase in the concentration of Cry3Aa, but the difference was not significant. When the Cry3Aa concentration reached $200 \mu\text{g ml}^{-1}$, the survival rates of cells expressing EGFP and RfAPNs were approximately 85% (fig. 7a). After incubation with 200 g ml^{-1} Cry3Aa for 2 h, although the cells expressing RfAPN2a or RfAPN2b showed slight deformation, neither the control nor the RfAPN-expressing cells showed significant cell swelling or fragmentation compared to the cells not incubated with the activated toxin (fig. 7b).

Discussion

Binding to specific receptors on BBMVs is crucial for the toxin to exert toxicity (Melo *et al.*, 2016). Many Cry3Aa receptors have been identified in Coleopteran pests, including APN from *M. alternatus* and cadherin from *T. molitor* (Fabrick *et al.*, 2009;

Guo *et al.*, 2020). However, before this study, no Cry3Aa toxin receptor had been identified in the midgut of *R. ferrugineus*. Therefore, the binding proteins of Cry3Aa in *R. ferrugineus*, including the V-type proton ATPase catalytic subunit, the GTP-binding protein and APN, were identified using pull-down assays. V-type proton ATPase catalytic subunits play essential roles in ATPase assembly and regulation of catalytic activity (Forgac, 1999). The V-type proton ATPase catalytic subunit in *M. alternatus* has also been found to bind to the Cry3Aa toxin; however, the mechanism of this interaction is still unclear (Guo *et al.*, 2020). GTP-binding proteins are peripheral proteins anchored to the plasma membrane by fatty acid chains (Ridley and Hall, 1992). They regulate growth factors and activate NADPH oxidase (Abo *et al.*, 1991; Ridley *et al.*, 1992). Notably, APN, a membrane protein that was first identified as a Cry receptor, is essential for Cry toxins to act on lepidopteran and dipteran pests (Takesue *et al.*, 1992; Batool *et al.*, 2019; Sun *et al.*, 2020). However, few studies have been conducted on the binding of Cry to APNs in Coleoptera. In this study, we identified two APN-binding APN proteins Cluster-7879.9674 (RfAPN2a) and Cluster-7879.8243 (RfAPN2b), belonging to the APN2 family. The dissociation constant (K_d) of activated Cry3Aa toxin to RfAPN2a and RfAPN2b was 108.5 and 68.2 nM, which is higher than Cry3Aa toxin to APN in *M. alternatus* (57 nM) (Guo *et al.*,

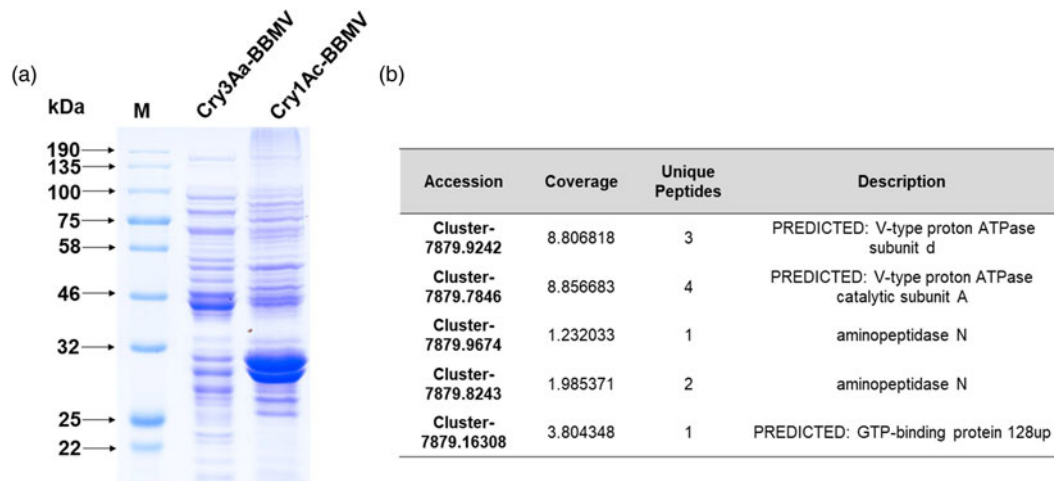


Figure 2. Protein pull-down and identification of Cry3Aa-binding proteins. (a) Cry3Aa toxin pull-down assays from *Rhynchochorus ferrugineus* BBMVs, Cry1Ac toxin was used as a control. (b) Mass spectrometry identification of the Cry3Aa-binding proteins from BBMVs.

2020). These results indicated that RfAPN2a and RfAPN2b were the binding proteins of Cry3Aa toxin in the BBMVs of *R. ferrugineus*.

Cry toxins bind to APN receptors via a glycosylation-mediated pathway; for example, Cry1Ac binds specifically by recognizing

different GalNAc sites on the receptors of *M. sexta*, *Heliothis virescens* and *Helicoverpa armigera*, indicating the importance of glycosylation site (Luo *et al.*, 1997; Jenkins *et al.*, 2000). Bioinformatics analyses showed that both RfAPN2a and RfAPN2b had potential *N*- and *O*-glycosylation sites, which

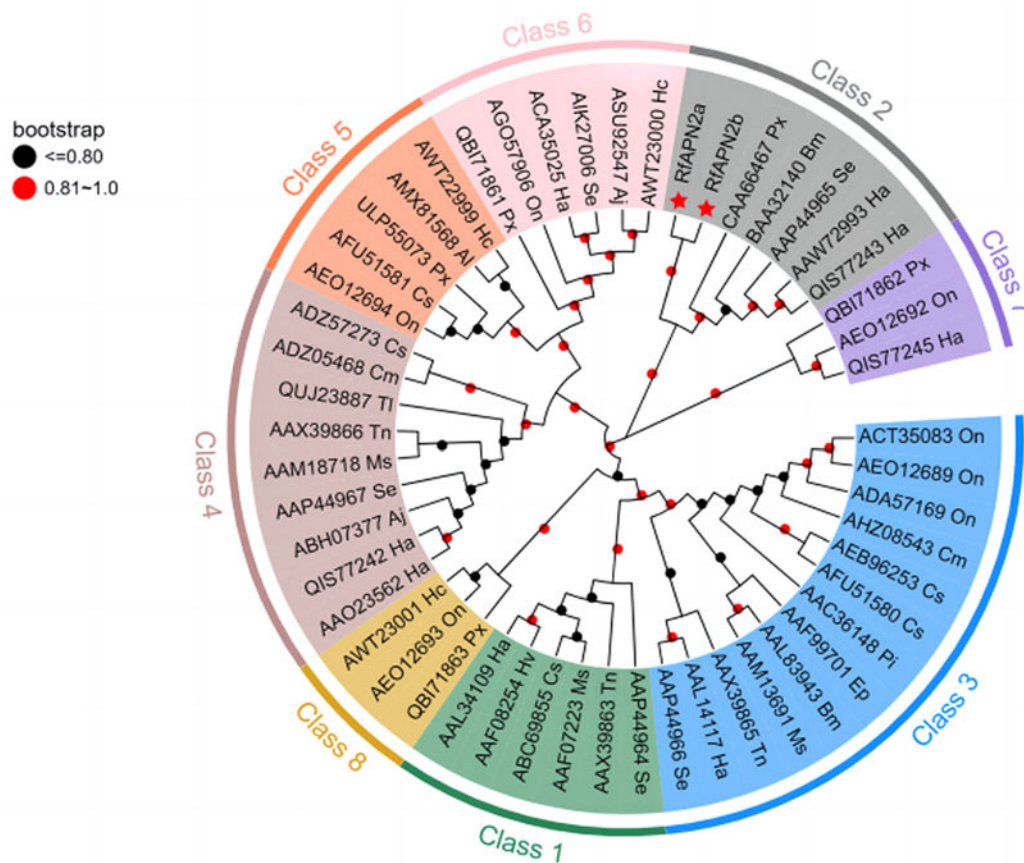


Figure 3. Neighbour-joining distance-based phylogenetic tree of APN proteins. The accession numbers of each amino acid sequence were indicated. Species abbreviations are as follows: Ha, *Helicoverpa armigera*; On, *Ostrinia nubilalis*; Se, *Spodoptera exigua*; Cs, *Chilo suppressalis*; Px, *Plutella xylostella*; Tn, *Trichoplusia ni*; Hc, *Hyphantria cunea*; Ms, *Manduca sexta*; Aj, *Achaea janata*; Cm, *Cnaphalocrocis medinalis*; Bm, *Bombyx mori*; Hv, *Heliothis virescens*; Al, *Athetis lepigone*; Pi, *Plodia interpunctella*; TL, *Telchin licus licus*; Ep, *Epiphyas postvittana*.

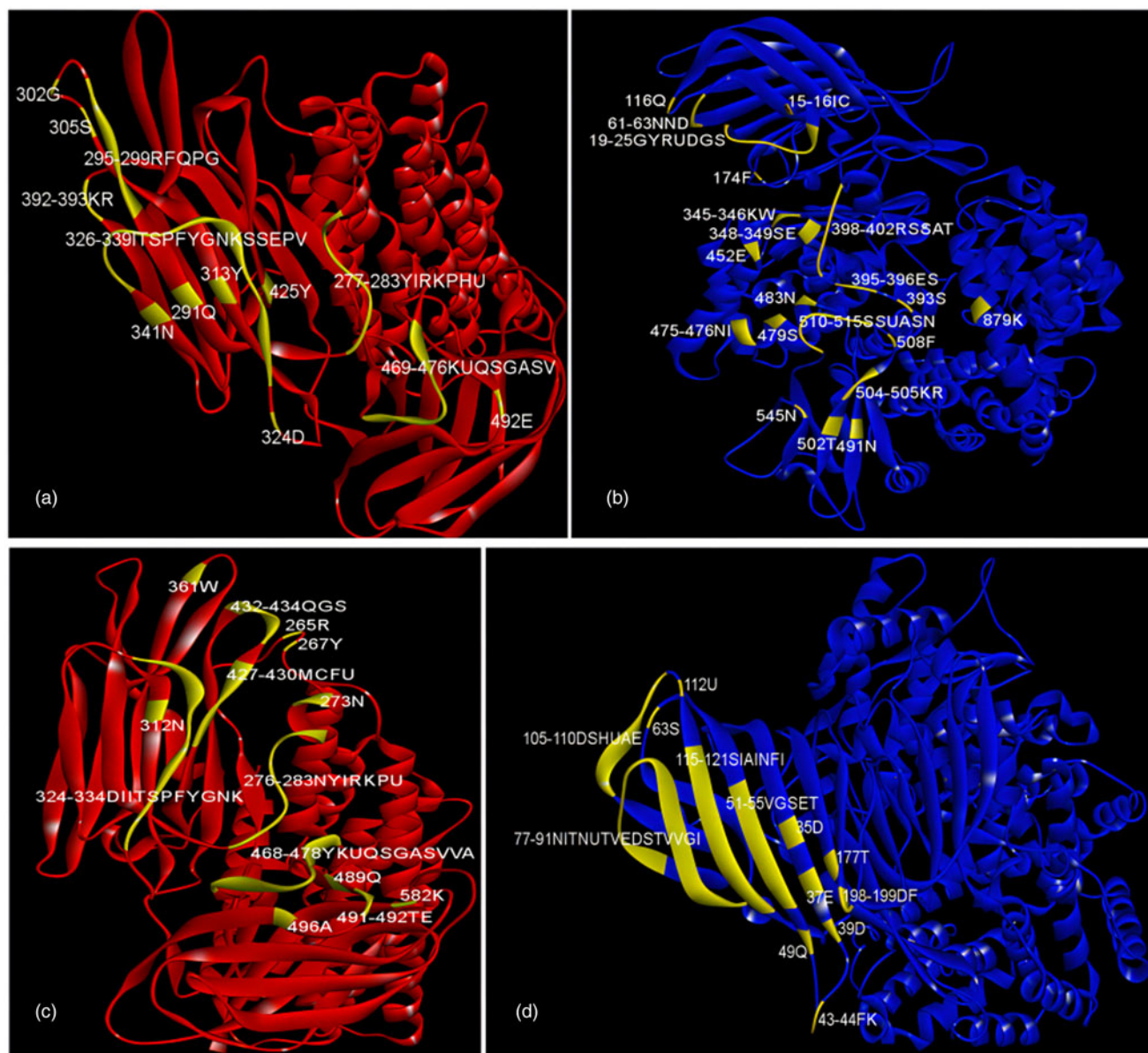


Figure 4. Molecular docking analysis of Cry3Aa with RfAPN2a and RfAPN2b. (a) Binding sites of Cry3Aa to RfAPN2a. (b) Binding sites of RfAPN2a to Cry3Aa. (c) Binding sites of Cry3Aa to RfAPN2b. (d) Binding sites of RfAPN2b to Cry3Aa. Yellow amino acid residues are the binding sites.

may be relevant for susceptibility to toxins. In addition, molecular docking results showed that Cry3Aa-binding sites were located in domains II and III. Domain II is involved in midgut receptor recognition, irreversible binding and membrane insertion, whereas domain III recognizes and binds to the receptor glycosylation sites (de Maagd *et al.*, 1999; Pardo-López *et al.*, 2013).

The mechanism of action underlying Cry toxicity is highly complex and two models have been proposed to explain it: the sequential binding model and the signalling pathway model (Vílchez, 2020). According to the sequential binding model, the activated toxin reversibly binds to the APN and ALP receptors. Then, the binding to the extracellular cadherin-like receptor is facilitated with high affinity to promote helix $\alpha 1$ proteolysis and form pre-pore toxin oligomers (Gómez *et al.*, 2002; Pacheco *et al.*, 2009). Oligomers display a high affinity for APN and ALP, leading to pore formation in membrane lipid rafts and osmotic cell death (Bravo *et al.*, 2004). Furthermore, this model

is supported by the finding that Cry toxins can still form oligomers *in vitro* without cadherin after removing helical $\alpha 1$ (Mario *et al.*, 2007). In the signalling pathway model, APN and cadherin proteins are often considered functional receptors, and after proteolytic activation, the toxin binds with high affinity to them, activating Mg^{2+} -dependent cell apoptosis (Zhang *et al.*, 2005, 2008; Vachon *et al.*, 2012). Therefore, APN receptors are indispensable in both Cry toxin models. In *R. ferrugineus*, RfAPN2a and RfAPN2b were expressed in HEK 293T cells, and cytotoxicity assays showed that the transgenic cells were not susceptible to activated Cry3Aa. This phenomenon has been previously observed for a *Heliothis virescens* cadherin-like protein that binds Cry1Fa to S2 cells but does not promote cytotoxicity (Jurat-Fuentes and Adang, 2006). These results suggest that Cry3Aa is not functional when binding to RfAPN2a and RfAPN2b alone and needs to interact with other midgut receptors to enhance the binding affinity in *R. ferrugineus* to effectively

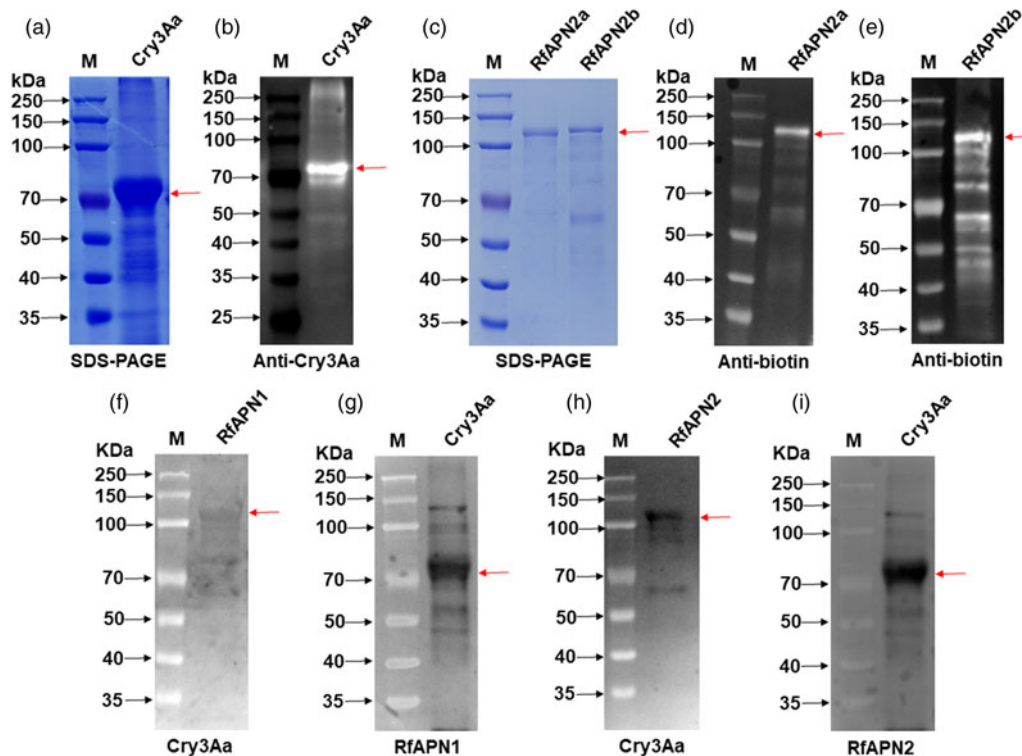


Figure 5. The interactions between Cry3Aa and recombinant RfAPNs. (a and b) SDS-PAGE and western blot analysis of the Cry3Aa crystal protein. (c, d and e) SDS-PAGE and western blot analysis of the GST-RfAPN2a and GST-RfAPN2b fusion proteins. (f) Cry3Aa was detected by far-western blot after probing with RfAPN2a. (g) RfAPN2a was detected by far-western blot after probing with Cry3Aa. (h) Cry3Aa was detected by far-western blot after probing with RfAPN2b. (i) RfAPN2b was detected by far-western blot after probing with Cry3Aa. The red arrow indicates the size of the target protein.

exert toxicity. However, in contrast to our conclusion, Wolfersberger (1990) reported that Cry1Ac was less toxic to gypsy moth larvae than Cry1Ab despite having a relatively stronger binding affinity to the receptors on BBMV, which was correlated with the kinetics of reversible and irreversible binding (Wolfersberger, 1990; Liang *et al.*, 1995). Therefore, further investigations are necessary to clarify the precise mechanism of action of Cry3Aa in *R. ferrugineus*.

Furthermore, modified Cry3Aa toxins can be used to control *R. ferrugineus*. It is likely that a Cry1Ac-garlic lectin fusion

toxin was synthesized and could bind to more receptors on the BBMV of *H. armigera*, leading to a 30-fold increase in insecticidal activity (Tajne *et al.*, 2013). We also found that the glycosylation and docking sites partially overlapped in RfAPNs. These binding sites could be further cloned or mutated to explore the binding mechanism between Cry3Aa and its receptors in *R. ferrugineus* (Kaur *et al.*, 2014). Therefore, modifying Cry3Aa to enhance the binding ability to the receptors in *R. ferrugineus* to induce toxicity is a feasible approach. Overall, this study demonstrates that RfAPN2a and RfAPN2b are putative Cry3Aa-binding

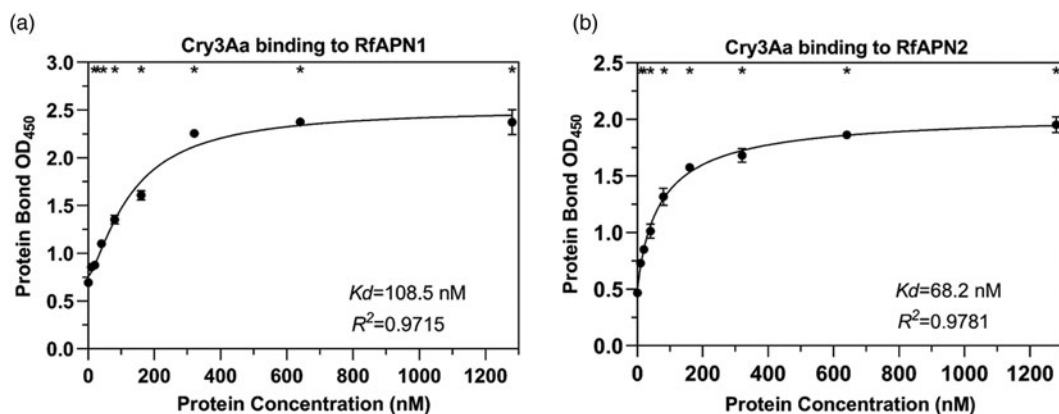


Figure 6. Binding affinity of Cry3Aa toxin to RfAPN2a and RfAPN2b of *Rhynchophorus ferrugineus*. The specific binding of Cry3Aa toxin to RfAPN2a (a) and RfAPN2b (b) was determined in the presence of increasing concentrations of Cry3Aa toxin. Each point represents the mean of three repeated measurements $OD_{450} \pm SEM$, and the curves are a four-parameter fitting curve. An asterisk indicates a significant difference at $P < 0.05$.

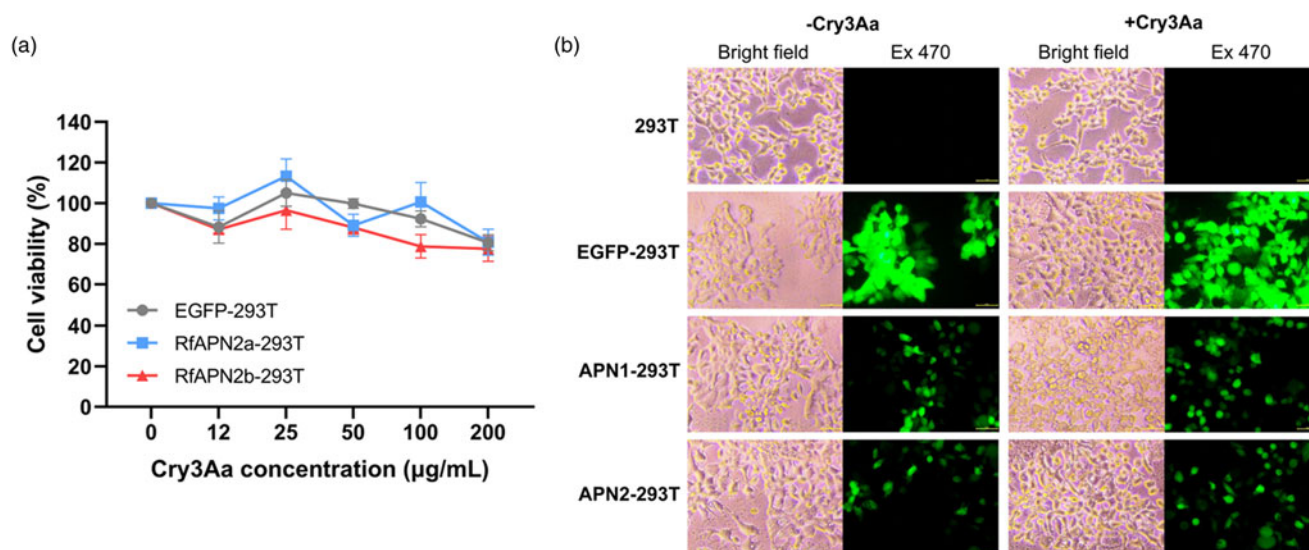


Figure 7. Effect of the trypsin-activated Cry3Aa toxin on cell viability. (a) Detection of transfected cells activity treated with Cry3Aa toxin by MTT assay. Each point represents the mean of three repeated measurements \pm SEM. (b) Morphological changes of 293T cells treated with 200 $\mu\text{g ml}^{-1}$ Cry3Aa. EGFP-293T refers to 293T cells transfected with the pQCMV vector. APN2a-293T refers to cells expressing RfAPN2a; APN2b-293T refers to cells expressing RfAPN2b. Ex 470 refers to the observation of cells under 470 nm excitation light.

proteins in *R. ferrugineus* and further provide a reasonable basis for controlling *R. ferrugineus* using *B. thuringiensis*.

Supplementary material. The supplementary material for this article can be found at <https://doi.org/10.1017/S0007485323000299>.

Acknowledgements. This work was supported by the National Natural Science Foundation of China (grant numbers U1905201 and 32171805); National Key R & D Program of China (grant number 2021YFD1400900); National Major Emergency Science and Technology Program of China (grant number ZD202001); Forestry Key Program of Science and Technology in Fujian Province (grant number 2021FKJ03); Natural Science Foundation of Fujian Province, China (grant number 2021J01056); Forestry Programs of Science and Technology in Fujian Province (grant number Mincaizhi [2020] 601); Science and Technology Program of Fujian Province (grant number 2018N5002); Forestry Science Research Project of Fujian Forestry Department (grant number Minlinke [2017] 03); Forestry Peak Discipline Construction Project of Fujian Agriculture and Forestry University (grant number 72202200205); Forest Science Peak Project of College of Forestry, Fujian Agriculture and Forestry University (grant number 71201800720); and Undergraduate Training Program for Innovation and Entrepreneurship of China (grant numbers 202210389029, X202210389174 and X202210389176).

Conflict of interest. The authors declare that they have no known competing financial interests or personal relationships that could have appeared to influence the work reported in this paper.

References

- Abo A, Pick E, Hall A, Totty N, Teahan CG and Segal AW (1991) Activation of the NADPH oxidase involves the small GTP-binding protein p21rac1. *Nature* **353**, 668–670.
- Adang MJ, Crickmore N and Jurat-Fuentes JL (2014) Diversity of *Bacillus thuringiensis* crystal toxins and mechanism of action. *Advances in Insect Physiology* **47**, 39–87.
- Al-Ayedh H (2008) Evaluation of date palm cultivars for rearing the red date palm weevil, *Rhynchophorus ferrugineus* (Coleoptera: Curculionidae). *Florida Entomologist* **91**, 353–358.

- Batool K, Alam I, Jin L, Xu J, Wu C, Wang J, Huang E, Guan X, Yu XQ and Zhang L (2019) CTLGA9 interacts with ALP1 and APN receptors to modulate Cry11Aa toxicity in *Aedes aegypti*. *Journal of Agriculture and Food Chemistry* **67**, 8896–8904.
- Bozbuga R and Hazir A (2008) Pests of the palm (*Palmae* sp.) and date palm (*Phoenix dactylifera*) determined in Turkey and evaluation of red palm weevil (*Rhynchophorus ferrugineus* Olivier) (Coleoptera: Curculionidae). *Bulletin OEPP/EPPO Bulletin* **38**, 127–130.
- Bravo A, Gómez I, Conde J, Muñoz-Garay C, Sánchez J, Miranda R, Zhuang M, Gill SS and Soberón M (2004) Oligomerization triggers binding of a *Bacillus thuringiensis* Cry1Ab pore-forming toxin to aminopeptidase N receptor leading to insertion into membrane microdomains. *Biochimica et Biophysica Acta Biomembranes* **1667**, 38–46.
- Bravo A, Gill SS and Soberón M (2007) Mode of action of *Bacillus thuringiensis* Cry and Cyt toxins and their potential for insect control. *Toxicon* **49**, 423–435.
- Bravo A, Likitvivanavong S, Gill SS and Soberón M (2011) *Bacillus thuringiensis*: a story of a successful bioinsecticide. *Insect Biochemistry and Molecular Biology* **641**, 423–431.
- Bravo A, Gómez I, Porta H, García-Gómez BI, Rodríguez-Almazan C, Pardo L and Soberón M (2013) Evolution of *Bacillus thuringiensis* Cry toxins insecticidal activity. *Microbial Biotechnology* **6**, 17–26.
- Chen, L (2016) Study on aggregation pheromone core-inducer and field application of red palm weevil. *China Tropical Agriculture* **3**, 37–39.
- Chen R and Weng Z (2002) Docking unbound proteins using shape complementarity, desolvation, and electrostatics. *Proteins: Structure, Function and Genetics* **47**, 281–294.
- Crickmore N, Berry C, Panneerselvamb S, Mishra R, Connor TR and Bonning BC (2021) A structure-based nomenclature for *Bacillus thuringiensis* and other bacteria-derived pesticidal proteins. *Journal of Invertebrate Pathology* **186**, 107438.
- de Maagd RA, Bakker PL, Masson L, Adang MJ, Sangadala S, Stiekema W and Bosch D (1999) Domain III of the *Bacillus thuringiensis* delta-endotoxin Cry1Ac is involved in binding to *Manduca sexta* brush border membranes and to its purified aminopeptidase N. *Molecular Microbiology* **31**, 463–471.
- Dembilio Ó, Jacas JA and Llácer E (2009) Are the palms *Washingtonia filifera* and *Chamaerops humilis* suitable hosts for the red palm weevil, *Rhynchophorus ferrugineus* (Col. Curculionidae)? *Journal of Applied Entomology* **133**: 565–567.

- de Oliveira JA, Negri BF, Hernández-Martínez P, Basso MF and Escribano B (2023) Mpp23Aa/Xpp37Aa insecticidal proteins from *Bacillus thuringiensis* (Bacillales: Bacillaceae) are highly toxic to *Anthonomus grandis* (Coleoptera: Curculionidae) larvae. *Toxins* **15**, 55.
- Einarson MB, Pugacheva EN and Orlinick JR (2007) Identification of protein-protein interactions with glutathione-S-transferase (GST) fusion proteins. *Csh Protocols* **2007**, pdb.top11.
- Fabrick J, Oppert C, Lorenzen MD, Morris K, Oppert B and Jurat-Fuentes, J.L (2009) A novel *Tenebrio molitor* cadherin is a functional receptor for *Bacillus thuringiensis* Cry3Aa toxin. *Journal of Biological Chemistry* **284**, 18401–18410.
- Forgas M (1999) Structure and properties of the vacuolar (H⁺)-ATPases. *Journal of Biological Chemistry* **274**, 12951–12954.
- Gómez I, Sánchez J, Miranda R, Bravo A and Soberón M (2002) Cadherin-like receptor binding facilitates proteolytic cleavage of helix K-1 in domain I and oligomer pre-pore formation of *Bacillus thuringiensis* Cry1Ab toxin. *FEBS Letter* **513**, 242–246.
- Güney G, Cedden D, Hänniger S, Heckel DG, Coutu C, Hegedus DD, Mutlu DA, Suludere Z, Sezen K, Güney E and Toprak U (2021) Silencing of an ABC transporter, but not a cadherin, decreases the susceptibility of Colorado potato beetle larvae to *Bacillus thuringiensis* ssp. *tenebrionis* Cry3Aa toxin. *Archives of Insect Biochemistry and Physiology* **108**, e21834.
- Guo CH, Zhao ST, Yuan M, Hu JJ and Lu MZ (2011) *Bacillus thuringiensis* Cry3Aa fused to a cellulase-binding peptide shows increased toxicity against the longhorned beetle. *Applied Microbiology Biotechnology* **93**, 1249–1256.
- Guo Y, Carballar-Lejarazú R, Sheng L, Fang Y, Wang S, Liang G, Hu X, Wang R, Zhang, F and Wu S (2020) Identification and characterization of aminopeptidase-N as a binding protein for Cry3Aa in the midgut of *Monochamus alternatus* (Coleoptera: Cerambycidae). *Journal of Economic Entomology* **113**, 2259–2268.
- Guo Y, Sun Y, Liao Q, Carballar-Lejarazú R, Sheng L, Wang S, Zhou J, Zhang F and Wu S (2021) Proteolytic activation of *Bacillus thuringiensis* Cry3Aa toxin in the red palm weevil (Coleoptera: Curculionidae). *Journal of Economic Entomology* **114**, 2406–2411.
- Han Z, Zhou J, Zhong F and Huang QL (2013) Research progress on damage and control of *Rhynchophorus ferrugineus*. *Guangdong Agricultural Sciences* **40**, 68–71.
- Huang ZH (2013) The occurrence and biological characters of red palm weevil, *Rhynchophorus ferrugineus* in Fujian, China. *Advanced Materials Research* **610–613**, 3552–3555.
- Ibrahim MA, Griko N, Junker M and Bulla LA (2010) *Bacillus thuringiensis*: a genomics and proteomics perspective. *Bioengineered Bugs* **1**, 31–50.
- Jenkins JL, Lee MK, Valaitis AP, Curtiss A and Dean DH (2000) Bivalent sequential binding model of a *Bacillus thuringiensis* toxin to gypsy moth Aminopeptidase N receptor. *Journal of Biological Chemistry* **275**, 14423–14431.
- Jurat-Fuentes JL and Adang MJ (2006) The *Heliothis virescens* cadherin protein expressed in *Drosophila* S2 cells functions as a receptor for *Bacillus thuringiensis* Cry1A but not Cry1Fa toxins. *Biochemistry* **45**, 9688–9695.
- Kaur R, Sharma A, Gupta D, Kalita M and Bhatnagar RK (2014) *Bacillus thuringiensis* toxin, Cry1C interacts with 128HLHFHLP134 region of aminopeptidase N of agricultural pest, Spodoptera litura. *Process Biochemistry* **49**, 688–696.
- Kumar S, Stecher G, Li M, Knyaz C and Tamura K (2018) MEGA X: molecular evolutionary genetics analysis across computing platforms. *Molecular Biology Evolution* **35**, 1547–1549.
- Liang Y, Patel S and Dean D (1995) Irreversible binding kinetics of *Bacillus thuringiensis* CryIA δ -Endotoxins to gypsy moth brush border membrane vesicles is directly correlated to toxicity. *Journal of Biological Chemistry* **270**, 24719–24724.
- Llácer E, Dembilio O and Jacas JA (2010) Evaluation of the efficacy of an insecticidal paint based on chlorpyrifos and pyriproxyfen in a microencapsulated formulation against *Rhynchophorus ferrugineus* (Coleoptera: Curculionidae). *Journal of Economic Entomology* **103**, 402–408.
- Luo KE, Sangadala S, Masson L, Mazza A, Brousseau R and Adang MJ (1997) Mediating specific *Bacillus thuringiensis* Cry1A-endotoxin binding and pore formation. *Insect Biochemistry and Molecular Biology* **27**, 735–743.
- Mario S, Liliana PL, Idalia L, Isabel G, Bruce ET and Alejandra B (2007) Engineering modified Bt toxins to counter insect resistance. *Science (New York, N.Y.)* **318**, 1640–1642.
- Melo ALDA, Soccol VT and Soccol CR (2016) *Bacillus thuringiensis*: mechanism of action, resistance, and new applications: a review. *Critical Reviews in Biotechnology* **36**, 317–326.
- Pacheco S, Gómez I, Arenas I, Saab-Rincon G, Rodríguez-Almazán C, Gill SS, Bravo A and Soberón M (2009) Domain II loop 3 of *Bacillus thuringiensis* Cry1Ab toxin is involved in a “Ping Pong” binding mechanism with *Manduca sexta* aminopeptidase-N and cadherin receptors. *Journal of Biological Chemistry* **284**, 32750–32757.
- Pardo-López L, Soberón M and Bravo A (2013) *Bacillus thuringiensis* insecticidal three-domain Cry toxins: mode of action, insect resistance and consequences for crop protection. *FEMS Microbiology Review* **37**, 3–22.
- Pérez C, Fernandez LE, Sun J, Folch JL, Gill SS, Soberón M and Bravo A (2005) *Bacillus thuringiensis* subsp. *israelensis* Cyt1Aa synergizes Cry11Aa toxin by functioning as a membrane-bound receptor. *Proceedings of the National Academy of Sciences U S A* **102**, 18303–18308.
- Ridley AJ and Hall A (1992) The small GTP-binding protein rho regulates the assembly of focal adhesions and actin stress fibers in response to growth factors. *Cell* **70**, 389–399.
- Ridley AJ, Paterson HF, Johnston HF, Diekmann D and Hall A (1992) The small GTP-binding protein rac regulates growth factor-induced membrane ruffling. *Cell* **70**, 401–410.
- Sato R, Adegawa S, Li X, Tanaka S and Endo H (2019) Function and role of ATP-binding cassette transporters as receptors for 3D-cry toxins. *Toxins* **11**, 124.
- Schnepf E, Crickmore N, van Rie J, Lereclus D, Baum J, Feitelson J, Zeigler DR and Dean DH (1998) *Bacillus thuringiensis* and its pesticidal crystal proteins. *Microbiology and Molecular Biology Reviews* **62**, 775–806.
- Soberón M, Portugal L, Garcia-Gómez BI, Sánchez J, Onofre J, Gómez I, Pacheco S and Bravo A (2018) Cell lines as models for the study of Cry toxins from *Bacillus thuringiensis*. *Insect Biochemistry and Molecular Biology* **93**, 66–78.
- Subramanian B, Gao S, Lercher MJ, Hu S and Chen WH (2019) Evolvview v3: a webserver for visualization, annotation, and management of phylogenetic trees. *Nucleic Acids Research* **47**, W270–W275.
- Sun Y, Yang P, Jin H, Liu H, Zhou H, Qiu L, Lin Y and Ma W (2020) Knockdown of the aminopeptidase N genes decreases susceptibility of *Chilo suppressalis* larvae to Cry1Ab/Cry1Ac and Cry1Ca. *Pesticide Biochemistry and Physiology* **162**, 36–42.
- Tajne S, Boddupally D, Sadumpati V, Vudem DR and Khareedu VR (2013) Synthetic fusion-protein containing domains of Bt Cry1Ac and *Allium sativum* lectin (ASAL) conferred enhanced insecticidal activity against major lepidopteran pests. *Journal of Biotechnology* **171**, 71–75.
- Takesue S, Yokota K, Miyajima S, Taguchi R and Takesue Y (1992) Partial release of aminopeptidase N from larval midgut cell membranes of the silkworm, *Bombyx mori*, by phosphatidylinositol-specific phospholipase C. *Comparative Biochemistry and Physiology* **102**, 7–11.
- Tsuda Y, Nakatani F, Hashimoto K, Ikawa S, Matsuura C, Fukada T, Sugimoto K and Himeno M (2003) Cytotoxic activity of *Bacillus thuringiensis* Cry proteins on mammalian cells transfected with cadherin-like Cry receptor gene of *Bombyx mori* (silkworm). *Biochemical Journal* **369**, 697–703.
- Vachon V, Laprade R and Schwartz JL (2012) Current models of the mode of action of *Bacillus thuringiensis* insecticidal crystal proteins: a critical review. *Journal of Invertebrate Pathology* **111**, 1–12.
- Vilchez S (2020) Making 3D-cry toxin mutants: much more than a tool of understanding toxins mechanism of action. *Toxins* **12**, 600.
- Wang Q, Zuo Z, Wang X, Gu L, Yoshizumi T, Yang Z, Yang L, Liu Q, Liu W and Han YJ (2016) Photoactivation and inactivation of Arabidopsis cryptochrome 2. *Science (New York, N.Y.)* **354**, 343–347.

- Wolfersberger M** (1990) The toxicity of two *Bacillus thuringiensis* δ -endotoxins to gypsy moth larvae is inversely related to the affinity of binding sites on midgut brush border membranes for the toxins. *Experientia* **46**, 475–477.
- Wolfersberger M, Luethy P, Maurer A, Parenti P, Sacchi FV, Giordana B and Hanozett GM** (1987) Preparation and partial characterization of amino acid transporting brush border membrane vesicles from the larval midgut of the cabbage butterfly (*Pieris brassicae*). *Comparative Biochemistry and Physiology* **86**, 301–308.
- Zhang X, Candas M, Griko NB, Rose-Young L and Bulla LA** (2005) Cytotoxicity of *Bacillus thuringiensis* Cry1Ab toxin depends on specific binding of the toxin to the cadherin receptor BT-R1 expressed in insect cells. *Cell Death & Difference* **12**, 1407–1416.
- Zhang R, Hua G, Andacht TM and Adang MJ** (2008) A 106-kDa aminopeptidase is a putative receptor for *Bacillus thuringiensis* Cry11Ba toxin in the mosquito *Anopheles gambiae*. *Biochemistry* **47**, 11263–11272.